The Chest Wall

2

Gebhard Mathis and Wolfgang Blank

The chest wall—with the exception of the parietal pleura behind the ribs—is well accessed by sonography because of its position immediately next to the ultrasound transducer (Sakai et al. 1990). Any suspicious findings on palpation of the chest (whether inflammatory or neoplastic) may be an indication for chest sonography. Quite often the subsequent procedure consists of sonographic control investigations and sonography-guided aspiration. Chest trauma is an excellent indication for sonography of the chest wall. Fractures of the rib and the sternum can be diagnosed with great accuracy. Concomitant conditions such as local hematoma, pleural effusion or pneumothorax can also be identified by sonography (Mathis 1997).

Indications for sonography of the chest wall:

- Pain
- Ambiguous findings on palpation
- Ambiguous X-ray findings
- Chest trauma
- Tumor staging
- Intervention
- Follow-up

G. Mathis (✉)
Internistische Praxis, Bahnhofstrasse 16/2, 6830 Rankweil, Austria
e-mail: gebhard.mathis@cable.vol.at

W. Blank
Klinikum am Steinenberg, Medizinische Klinik
Akademisches Lehrkrankenhaus der Universität Tübingen,
Steinenbergstraße 31, 72764 Reutlingen, Germany
e-mail: blank_w@kreiskliniken-reutlingen.de

Pathological sonography findings in the chest wall:

1. Soft tissue
   (a) Accumulation of fluid
      - Hematoma
      - Seroma
      - Lymphatic cyst
      - Abscess
   (b) Tumors
      - Lipoma
      - Fibroma
      - Sarcoma
      - Metastases
      - Invasion by carcinoma
   (c) Lymph nodes
      - Inflammatory lymph nodes
      - Malignant lymphoma
      - Lymph node metastases
2. Bone
   (a) Fractures
      - Ribs
      - Sternum
      - Clavicle
      - Scapula
   (b) Osteolysis—metastases
      - Bronchial carcinoma
      - Breast carcinoma
      - Prostate carcinoma
      - Multiple myeloma
      - Others

G. Mathis (ed.), *Chest Sonography,*
DOI 10.1007/978-3-642-21247-5_2, © Springer-Verlag Berlin Heidelberg 2011

2.1 Soft Tissue

2.1.1 Accumulation of Fluid

2.1.1.1 Hematoma

Depending on the erythrocyte content and the degree of organization—hence also depending on the age of the lesion—hematomas may be accompanied by various echo patterns. They are usually anechoic or hypoechoic (Fig. 2.1). Occasionally one finds fine, hazy central echoes. In rare cases there may be intermediate forms or denser echoes in the central region. Organized hematomas may have very inhomogeneous echoes.

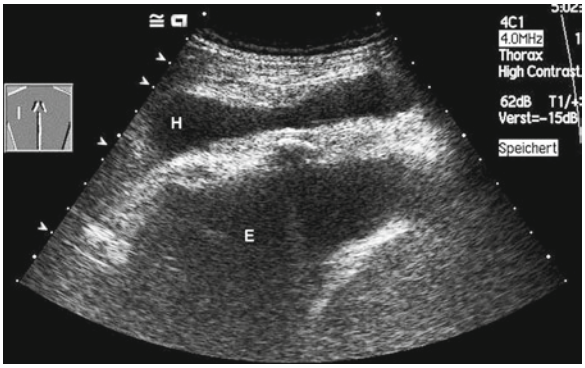

Fig. 2.1 A subcutaneous hematoma after blunt trauma (*H*). At this site the hematoma is largely anechoic. A large quantity of fluid in the pleural cavity (*E*) turns out to be a hemothorax on puncture

2.1.1.2 Seroma, Lymphatic Cyst

Postoperative seromas are largely anechoic, round or bizarre in shape and have no capsule. Lymphatic cysts are similar in terms of structure, usually round or oval. The occluded lymphatic vessel can be visualized (Fig. 2.2).

2.1.1.3 Abscess

The cellular and protein content of the cavity of an abscess may result in different central structures. The content of abscesses may be similar to that of hematomas. Differentiation may be difficult because intermediate stages such as infected hematomas may be present. Capsular formations of different degrees are an important distinction criterion for abscesses. Floating internal structures may be present (Fig. 2.3).

2.1.2 Tumors

2.1.2.1 Lipoma, Fibroma

The echogenicity of lipomas and fibromas depends on their cellular fat content, their connective tissue content, and impedance differences in interstitial tissue. The sonographic texture may vary from hypoechoic to relatively echodense forms and the lesions may be poorly demarcated from the surrounding tissue. A capsule may be present (Fig. 2.4).

2.1.2.2 Sarcomas, Soft-Tissue Metastases

Invasive growth is one of the main criteria of a malignant space-occupying lesion. The texture is usually hypoechoic and may be combined with inhomogeneous hyperechoic portions. Color-Doppler sonography may be useful for the assessment of hypoechoic structures suspected of malignancy. The type of vascularization and the course of the vessels may help to confirm a suspected malignant lesion (Figs. 2.5–2.8).

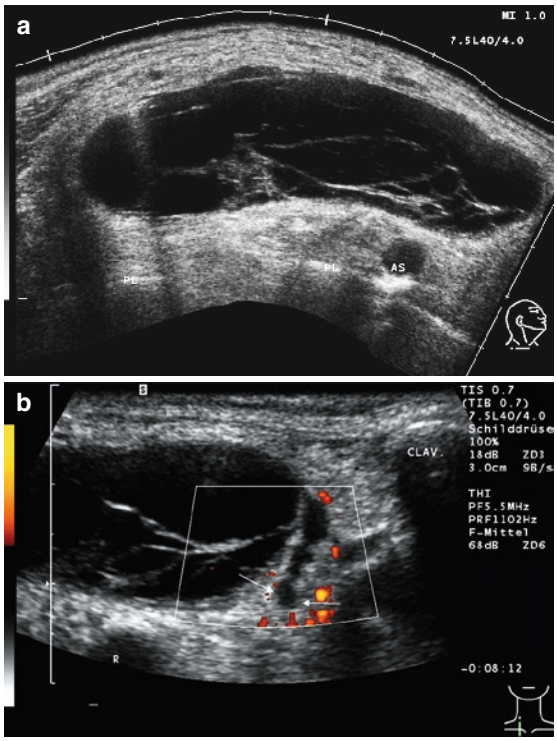

Fig. 2.2 Painful postoperative swelling in the lateral region of the neck on the left side. (**a**) Sonography reveals an echo-free, chambered space-occupying lesion measuring 10 cm × 4 3 cm in size. (**b**) An occluded lymph tract (*arrows*)

Knowledge of the vascularization pattern is also very useful when performing sonography-guided aspiration. At

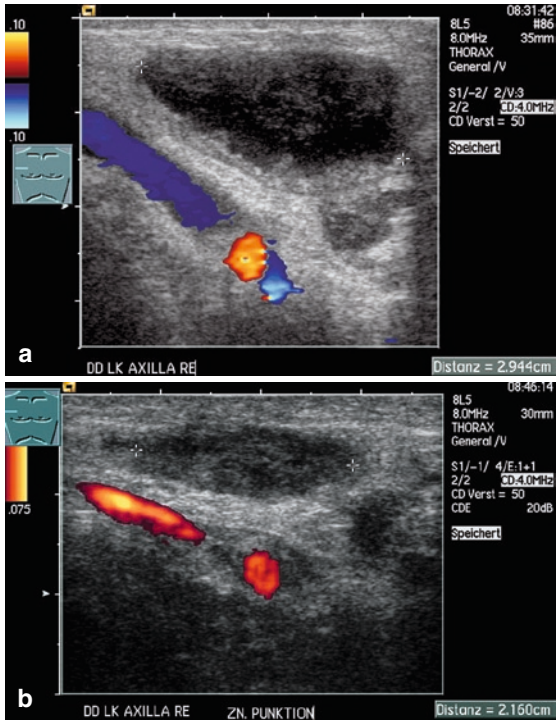

Fig. 2.3 A painful swelling in the region of the right axilla is indicative of a sweat gland abscess. (**a**) Sonography reveals a largely anechoic space-occupying lesion measuring 3 cm × 1.5 cm in size. The moderately echogenic margin is indicative of a starting capsular formation. (**b**) Sonography-guided aspiration yields pus. The residual fluid is absorbed

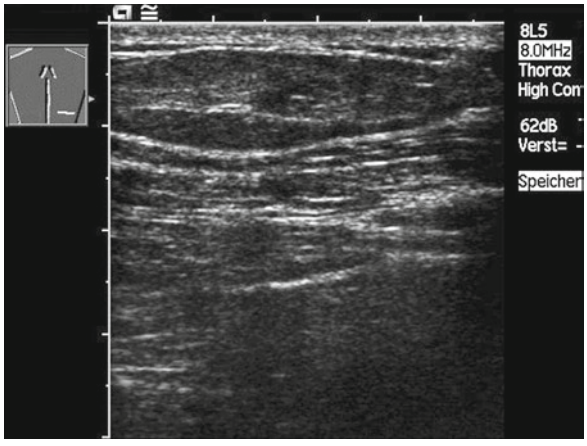

Fig. 2.4 Moderately echogenic lipoma in infrascapular location, with slightly blurred margins

this favorable location close to the transducer, sonography-guided aspiration is a most useful method to obtain histological material and finally to confirm the diagnosis.

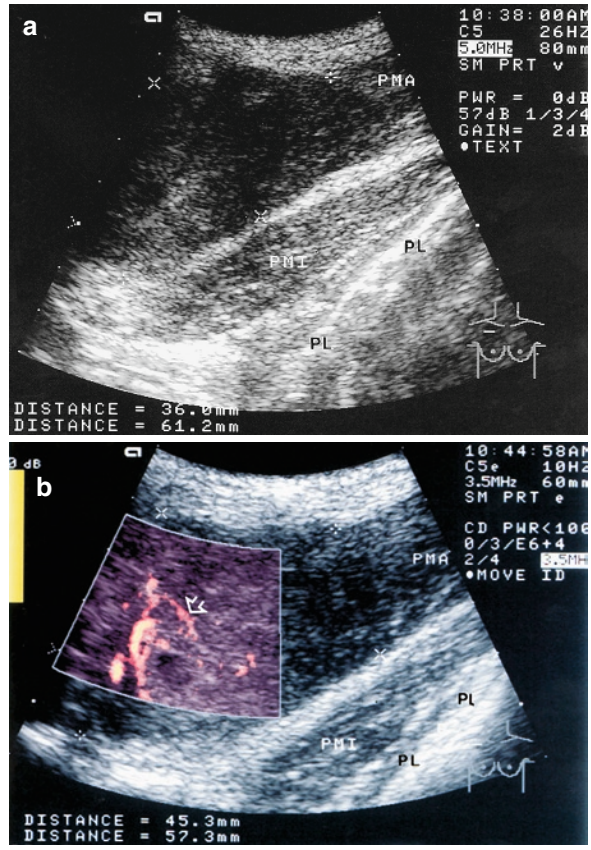

Fig. 2.5 (**a**) Muscle lymphoma. A 20-year-old man who experienced pain in the chest wall when exercising (bodybuilding). Clinical investigation showed hardening and swelling in the pectoral muscles on the right side. On sonography there was a hypoechoic transformation in the lateral portions of the pectoralis major muscle, which was interpreted as hemorrhage on B-mode sonography. (**b**) Evidence of a markedly vascularized lesion on color-Doppler sonography; atypical vessels (corkscrew, fluctuations in diameter, "high-velocity" signals). The surgical biopsy revealed a non-Hodgkin's lymphoma in the pectoral muscle

2.1.3 Lymph Nodes

Subcutaneous palpable swellings are usually caused by lymph nodes. The sonomorphology of lymph nodes is indicative of their origin and allows cautious assessment of the benign or malignant nature of the lesion when viewed in conjunction with the clinical condition. High-frequency probes yield a differentiated B-mode image. The vascularization pattern on color-Doppler sonography images provides further information about the type of lymph node (Bruneton et al. 1986; Hergan et al. 1994). The possibilities of assessing the benign or

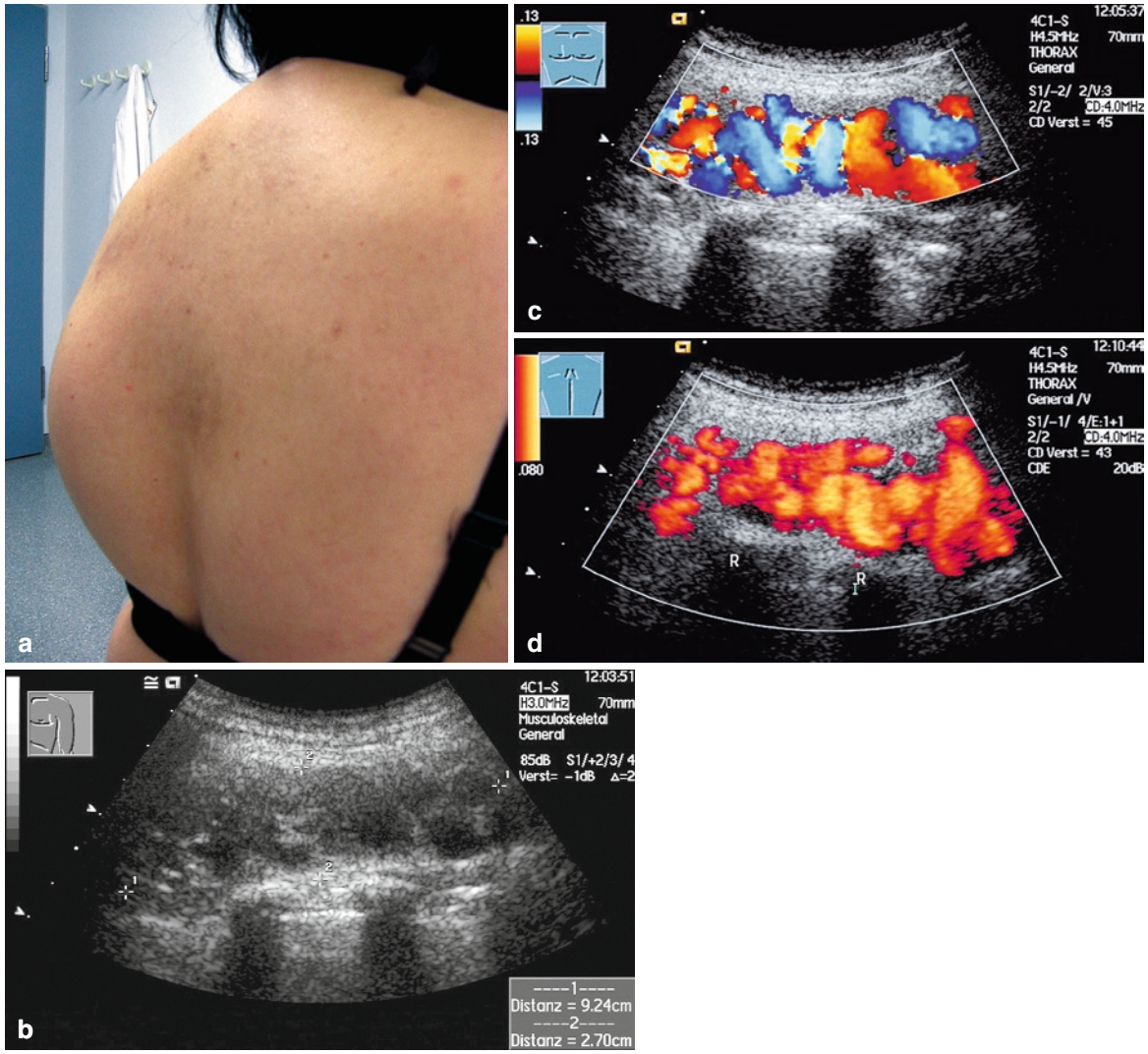

Fig. 2.6 (**a**) Hemangioma in the dorsal chest wall. Soft swelling on the left aspect of the spine; the swelling has been growing in the last few years. (**b**) Space-occupying lesion at the level of the scapula with no invasion of the surrounding structures. (**c**, **d**) The space-occupying lesion is of the vascular type; it is supplied and drained by paravertebral vessels

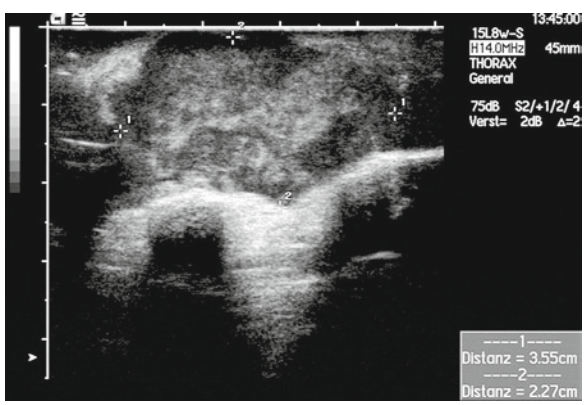

Fig. 2.7 Soft-tissue metastasis of a sarcoma

malignant nature of a lesion have been definitely improved by better resolution of the B-mode image as well as the use of various Doppler procedures to assess the pattern of vascularization (Chang et al. 1994; Tschammler et al. 1998; Table 2.1).

However, the benign or malignant nature of a lesion should be established with caution on the basis of sonomorphological criteria alone; the final assessment can only be made by histological confirmation of the diagnosis after aspiration or on the basis of disease progression. Changes in size and sonomorphology are of great significance in clinical practice. Thus, sonography controls may be used to confirm the diagnosis in

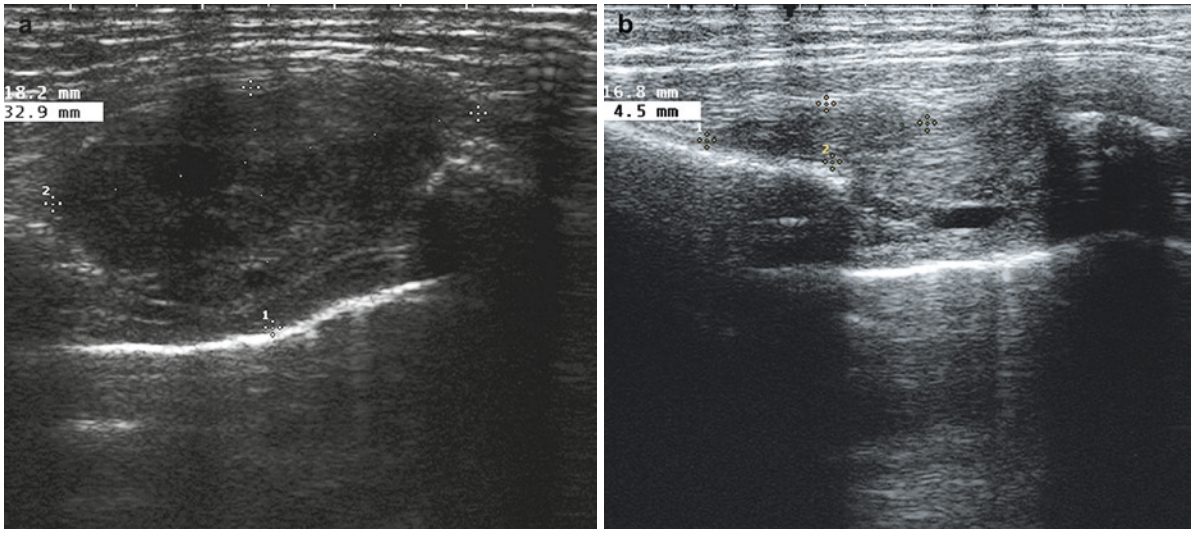

Fig. 2.8 (**a**) Solitary soft-tissue metastasis in parasternal location 15 years after breast carcinoma, confirmed by US-guided biopsy. (**b**) Resolution under radiotherapy

Table 2.1 Sonomorphology of lymph nodes

	Inflammatory	Malignant lymphoma	Lymph node metastasis
Morphology	Oval, longitudinal	Round, oval	Round
Margin	Smooth	Smooth	Irregular
Demarcation	Sharp	Sharp	Blurred
Growth	Bead-like	Expansive, displacing	Invasive
Mobility	Good	Good, moderate	Poor
Echogenicity	Hypoechoic margin "signs of hilar fat"	Hypoechoic, cystic	Inhomogeneous echoes
Vascularization	Regular, central	Irregular	Corkscrew-like

cases of inflammatory disease and to document the success of therapy in cases of malignant lymph nodes.

2.1.3.1 Inflammatory Lymph Nodes

Inflammatory lymph nodes seldom exceed 20 mm in size. Usually they have smooth margins, are oval, triangular or longitudinal in shape (Fig. 2.9). In cases of lymphadenitis, lymph nodes are typically arranged in a pearl-like fashion along the lymph node sites. In keeping with the anatomy, one frequently finds a more or less marked echogenic central zone which is termed a hilar fat sign, representing fat and connective tissue in the center of the lymph node. This sign is seen particularly during the healing phase of inflammatory processes (Fig. 2.10). The zone that is sharply demarcated from the surrounding tissue is hypoechoic. In this region one frequently finds vessels running a regular course on Doppler ultrasound images. The hilum of the lymph node with its arteries and veins is also visualized.

2.1.3.2 Malignant Lymphoma

A homogeneous, hypoechoic lesion with sharp margins is characteristic of malignant lymphoma. Centrocytic and Hodgkin's lymphomas are usually nearly anechoic in terms of structure and look like cysts in such cases. Malignant lymphomas may be round, tightly oval, or very rarely triangular in shape (Figs. 2.11 and 2.12). The presence of vessels on both sides (sandwich) is also indicative of a malignant lymphoma. Malignant lymphomas may be strongly vascularized, but the vascularization may be irregular in the margins.

!
Acutely inflammatory lymph nodes look very similar to malignant lymphoma

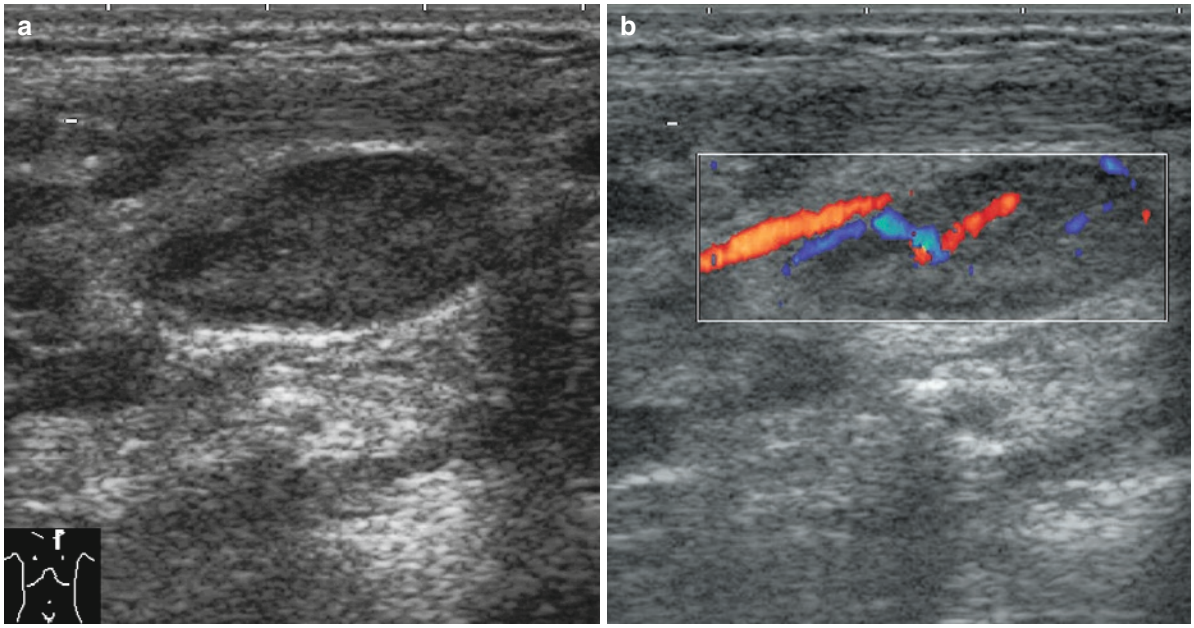

Fig. 2.9 Reactive inflammatory lymph node in the presence of listeriosis. (**a**) Hypoechoic margin, (**b**) regular perfusion

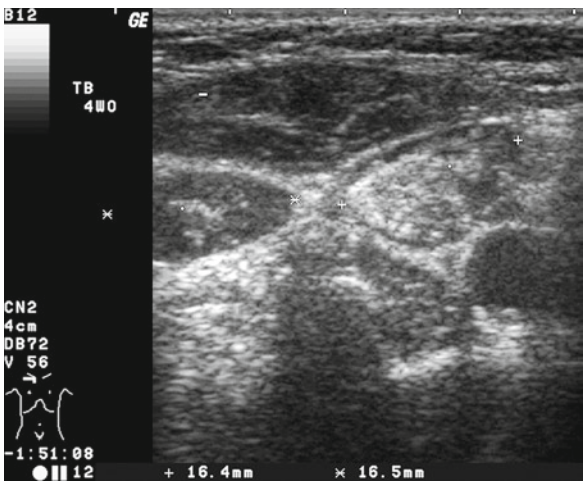

Fig. 2.10 Healing lymph node in the presence of tuberculosis. A narrow hypoechoic margin and a large echogenic center

2.1.3.3 Lymph Node Metastases

Lymph node metastases appear inhomogeneous on the ultrasound image. Moderately hyperechoic portions are often predominant. The demarcation to the surrounding tissue is usually blurred. Aggressive growth may be manifested as invasion of muscles and vessels (Gritzmann et al. 1990; Fig. 2.13). The size of lymph nodes is an unreliable criterion. However, metastases are more often larger than the maximum size of 20 mm achieved by inflammatory lymph nodes. Morphology is an important criterion. Metastatic lymph nodes tend to be round. One occasionally finds reactive lymph nodes in the vicinity of metastatic ones.

The vascularization pattern of lymph node metastases is typical: Vessels are frequently located at the margin, irregularly organized, run a chaotic course, flow in various directions, and tend to change their color (Tschammler et al. 2002).

Nonpalpable lymph nodes can also be visualized; therefore, sonography of the axilla is recommended for preoperative staging and monitoring the progress of breast carcinoma (Bruneton et al. 1984; Hergan et al. 1996; Fig. 2.14). Since recently the "sentinel lymph node" is also identified by sonography.

Currently, sonography is routinely demanded for staging a bronchial carcinoma because it is markedly superior to computed tomography in showing lymph node metastases in the supraclavicular groove (N3) and invasion of the chest wall (Suzuki et al. 1993). Nonpalpable lymph nodes are frequently discovered by this procedure (Fultz et al. 2002; van Overhagen et al. 2004, Prosch et al. 2007). Sonography discloses 17–36% more lymph nodes in this setting; in 3% the staging is upgraded. Further unnecessary investigations are avoided in about 10%. The cervical lymph nodes must be searched for because their presence indicates stage M1 disease.

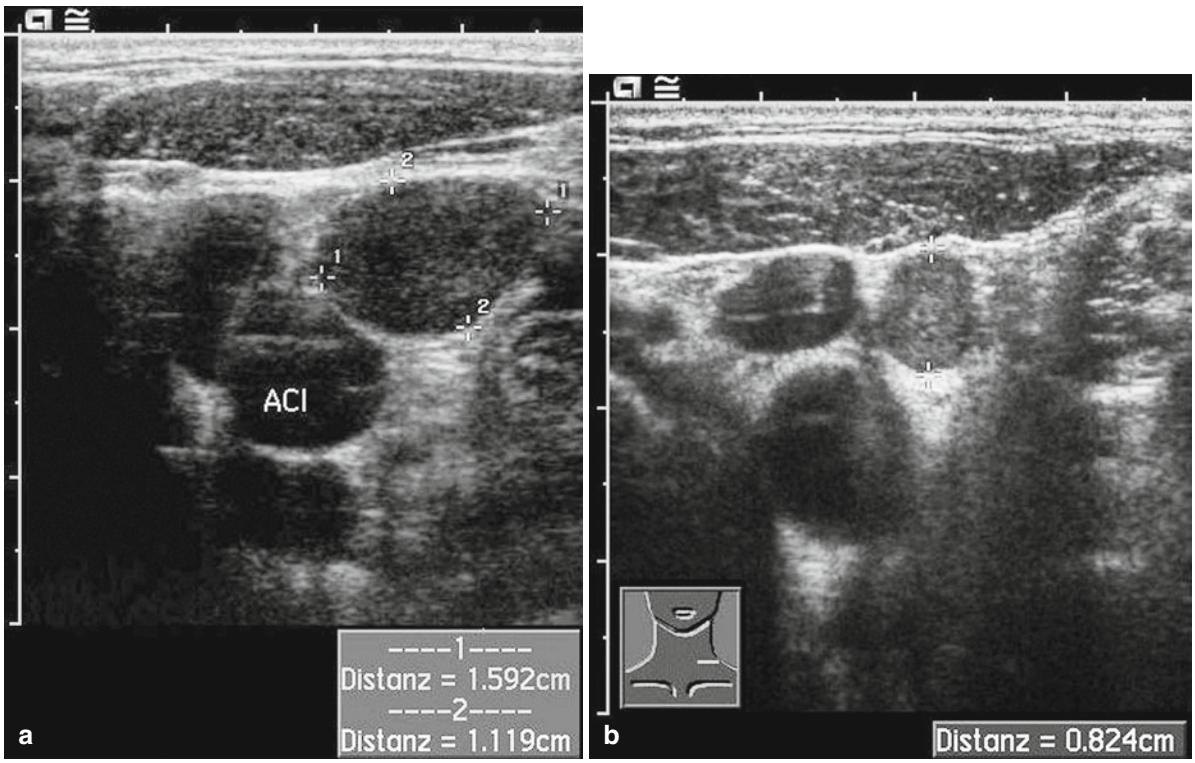

Fig. 2.11 Hodgkin's lymphoma. (**a**) At the time of diagnosis. (**b**) After three chemotherapy cycles. Reduced in size by more than 50%, then complete remission

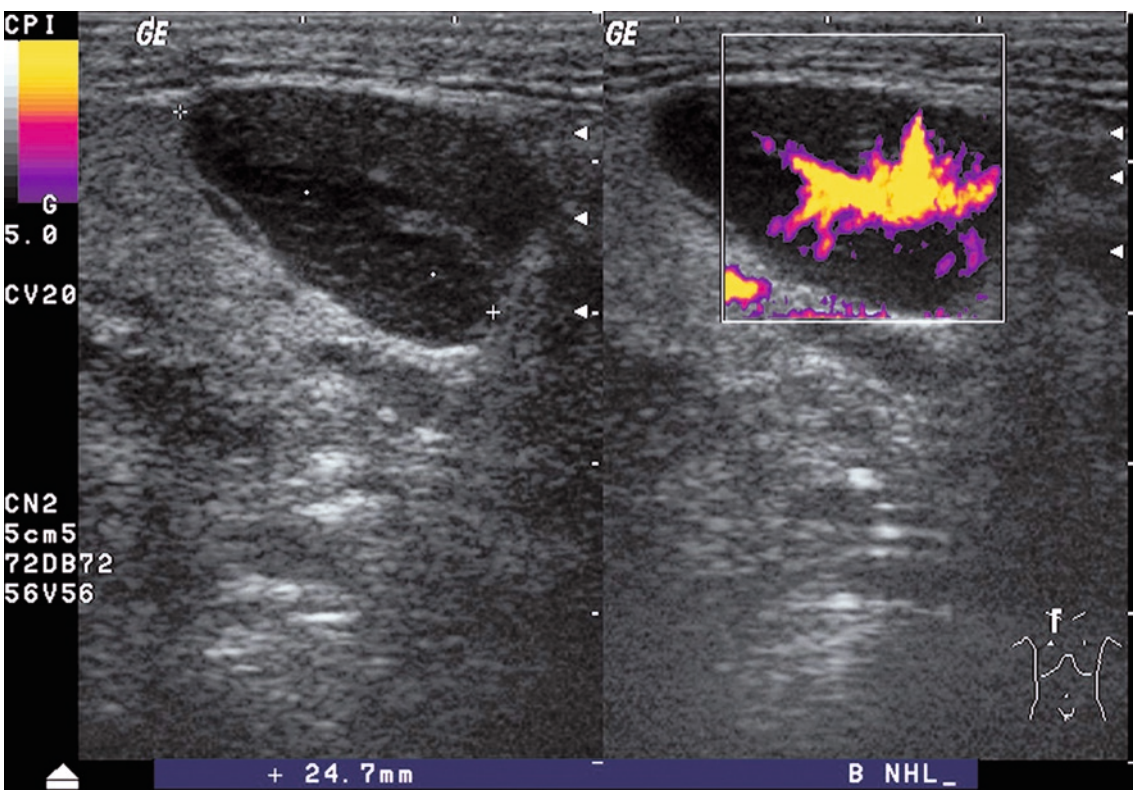

Fig. 2.12 B-cell chronic lymphocytic leukemia: hypoechoic lymph node with minimal hilar signs; strong and somewhat irregular vascularization

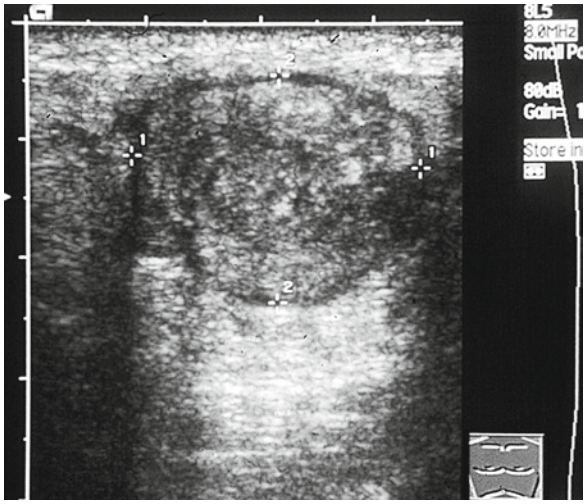

Fig. 2.13 Lymph node metastasis of an epidermoid lung carcinoma. Invasive growth into the vicinity. On palpation the mobility of the lesion was markedly reduced. The affected lymph node itself is characterized by inhomogeneous echoes, is onion-shaped in terms of structure, and invades its surroundings

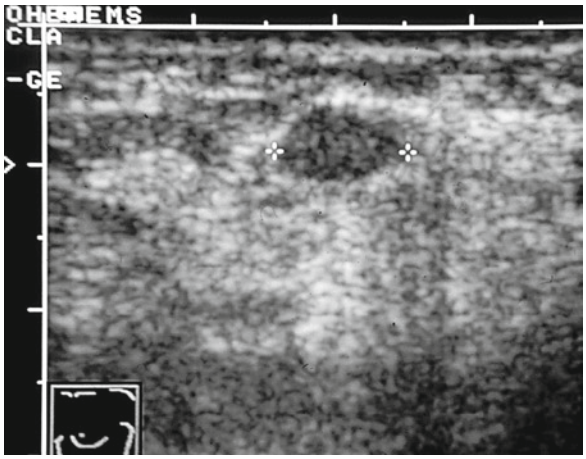

Fig 2.14 Nonpalpable axillary lymph node metastasis measuring 7 mm in size, in the presence of breast carcinoma

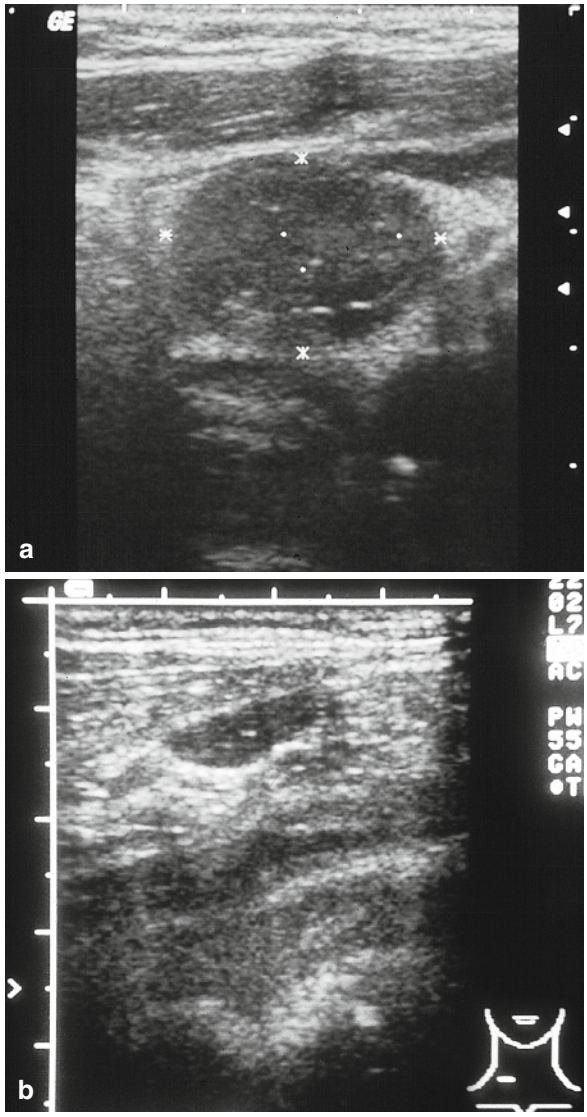

Fig. 2.15 (**a**) Cervical lymph node metastasis of a large-cell carcinoma of the lung. (**b**) After two cycles of chemotherapy this lymph node metastasis had resolved and now looks like a reactive lymph node

Ultrasound is also the most sensitive imaging procedure when the investigator is confronted with the question as to whether a tumor is invading the chest wall. For one thing, the resolution in the area of the soft tissues—using correspondingly high frequencies—is unexcelled to date. Furthermore, the dynamic investigation is able to show whether the tumor is breath dependent in terms of motion. Therefore, the current S-3 guidelines demand a sonography for staging in lung cancer (Goeckenjan et al. 2011).

Lymph node metastases are good parameters to monitor therapy. If the patient responds to chemotherapy or radiotherapy, reactive lymph nodes may persist (Fig. 2.15).

2.2 The Bony Chest

2.2.1 Fractures of the Ribs and the Sternum

Radiological diagnosis of the chest may prove difficult; nondislocated fractures are frequently not

Table 2.2 Sonography criteria for fractures of the ribs and the sternum

Direct signs	Concomitant indirect signs
At the site of pain	Hematoma
Cortical gap	Reverberation echoes/"chimney phenomenon"
Step in cortical bone	Pleural effusion
Dislocation	Pneumothorax
	Lung contusion lesions

seen. Lesions in the ribs and the sternum can be visualized well by sonography (Fenkl et al. 1992; Dubs-Kunz 1992; Dubs-Kunz 1996; Bitschnau et al. 1997; Table 2.2). The fracture gap, dislocation and bone fragments are directly visualized. Soft-tissue hematoma, fluid in the pleura and lung contusions are also seen (Wüstner et al. 2005).

The following procedure proved its worth in clinical practice: The patient points to the site of maximum pain. This area is investigated. Quite often a fracture can be diagnosed immediately at this site.

If the fracture gap is larger than the lateral resolution capacity of the ultrasound device, the gap is directly accessible to ultrasound diagnosis—which is usually the case. A nondislocated fracture can also be identified indirectly by reverberation echoes—the so-called chimney phenomenon. These reverberation artifacts occur at the margins of the fracture fragments and extend vertically in depth. In the absence of dislocation, the chimney phenomenon can be triggered by gentle pressure on the site of pain. Fractures in the rib and the sternum are characterized by the same sonomorphology. The criteria are direct evidence of a cortical gap or a cortical step (Fig. 2.16), and are indirect evidence of a local hematoma, a chimney phenomenon or an accompanying pleural effusion (Fig. 2.17).

Knowledge of the anatomy and anatomical variants is the most important requirement for assessment of the sternum. Thus, the usually discreet interruption of cortical bone in the region of synchondrosis between the corpus and the manubrium of the sternum should not be mistaken for a fracture. Besides, various possibilities of incorrect fusion of bones, which may occur in rare cases, should be taken into account (Fig. 2.18).

When monitoring the progression of disease one first finds a local hematoma as a hypoechoic/anechoic margin in the region of the fracture gap. Subsequent callus formation is marked by initial organization of

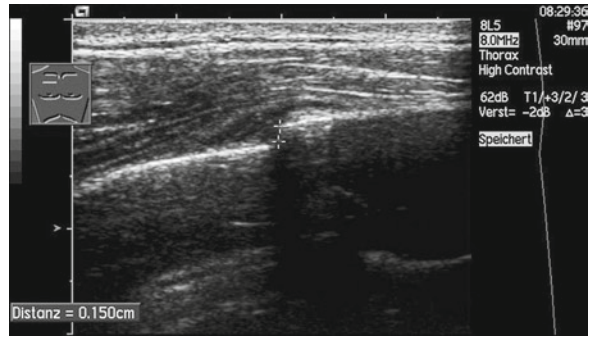

Fig. 2.16 Rib fracture with a step of 1.5 mm. This fracture could not be seen on X-rays. No accompanying hematoma above the fracture site

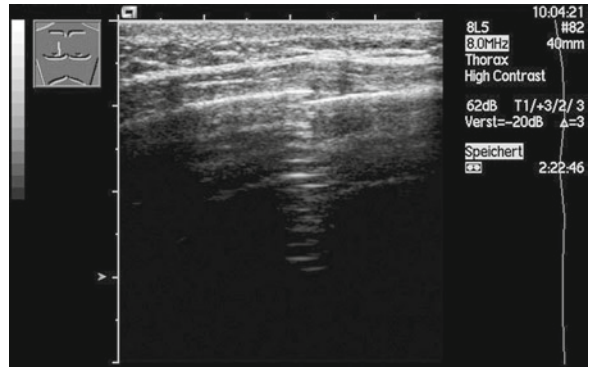

Fig. 2.17 Rib fracture with reverberation echoes, the "chimney phenomenon." In the absence of dislocation this phenomenon can be provoked by gentle pressure on the site of pain

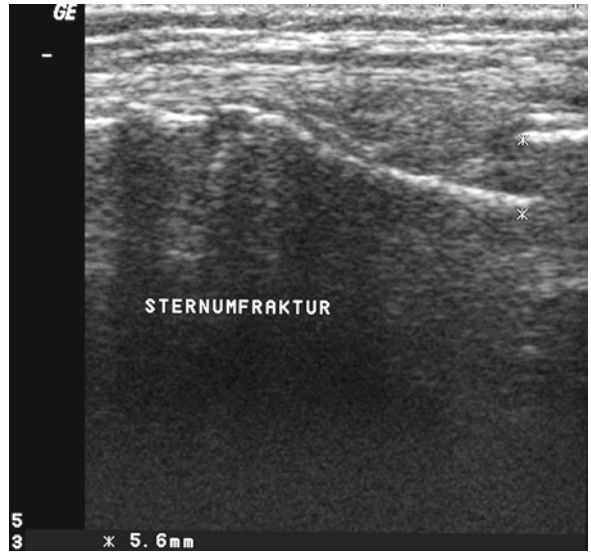

Fig. 2.18 *Right*: Fracture of the sternum after a rear-end collision (+ – +). *Left*: the uneven surface at the synchondrosis of the manubrium

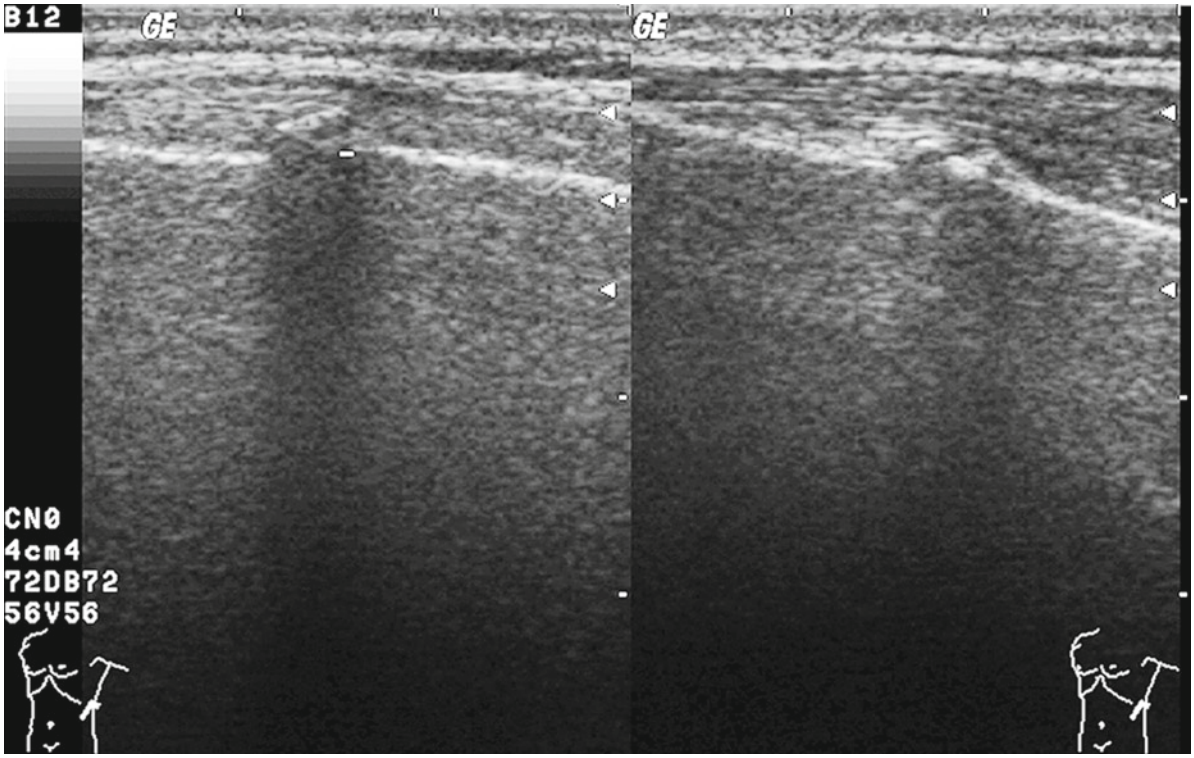

Fig. 2.19 Ten-week-old rib fracture. Recalcified uneven protrusion at the previous fracture site

the structure and thickening. The starting calcification causes fine acoustic shadows and may extend to complete ossification. Once ossification has occurred, one may find just a protrusion of the continuous, marked cortical reflex (Fig. 2.19). Healing disorders also can be easily identified by the absence of continuous ossification. Thickening starts from the third or fourth week after trauma. Complete restitution is usually achieved after a few months (Friedrich and Volkenstein 1994; Riebel and Nasir 1995).

The use of chest sonography is an increasing procedure in traumatology (Leitgeb et al. 1990; Mariacher Gehler and Michel 1994). As an adjunct to conventional X-rays, sonography provides significant additional information (Griffith et al. 1999). In a nonselected patient population with suspected rib fractures, sonography demonstrated twice as many fractures as did chest X-rays, including a targeted X-ray (Bitschnau et al. 1997). Sonography was particularly useful to assess the ventral region. In cases of rib fractures in conjunction with a fracture of the clavicle, however, conventional X-rays were superior.

For the patient it is very important to establish whether he/she has a chest contusion or a fracture because the two conditions have different consequences for his/her ability to work. In cases of severe chest trauma, the extent of an accompanying pleural effusion or hematoma or lung contusion (Fig. 2.20) can be rapidly and accurately estimated by sonography. Thus, the use of sonography is very meaningful in the emergency setting (Walz and Muhr 1990; Wischofer et al. 1995; Wüstner et al. 2005). However, a skin emphysema is a limitation for sonography (Fig. 2.21).

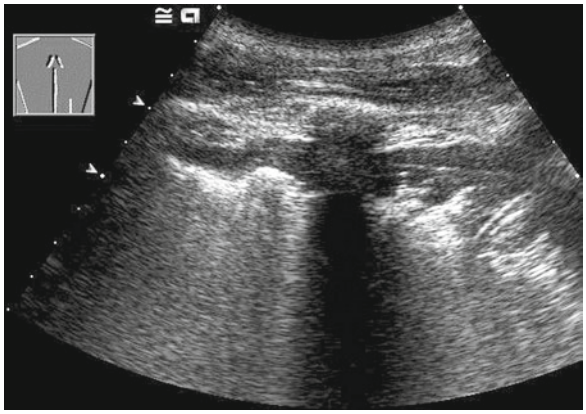

Fig. 2.20 Lung contusion: plate formed subpleural lung consolidation

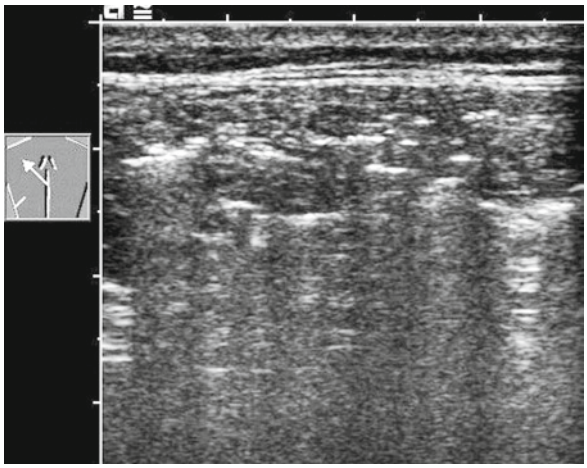

Fig. 2.21 Emphysema of the skin. Numerous subcutaneous air reflections greatly impair the image in terms of depth. The chest wall is not seen

2.2.2 Osteolysis

Osteolyses are usually metastases and are characterized by an interrupted and destroyed cortical reflex with pathological echo transmission (Fig. 2.22). Osteolytic metastases are usually seen as well-demarcated round or oval space-occupying lesions with a partly hypoechoic and a partly rough echo structure. Color-coded duplex sonography reveals corkscrew-like neoformation of vessels (Fig. 2.23).

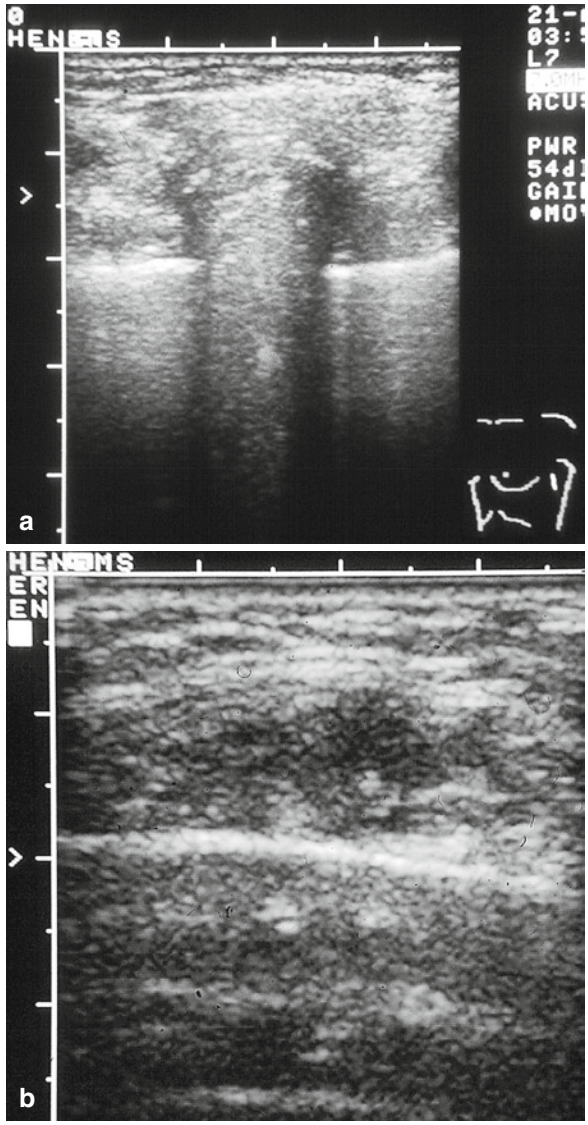

Fig. 2.22 (**a**) Cross section of an osteolytic rib metastasis in the presence of a pleuropulmonary adenocarcinoma. (**b**) Longitudinal section of the metastasis. The rib is raised, the cortical reflex largely destroyed, the echotexture of the metastasis is inhomogeneous. The pathological echo transmission also allows the pleura to be visualized

Sonography-guided aspiration is the procedure to be used if the clinician wishes to make a histological diagnosis of the osteolysis because osteolyses are

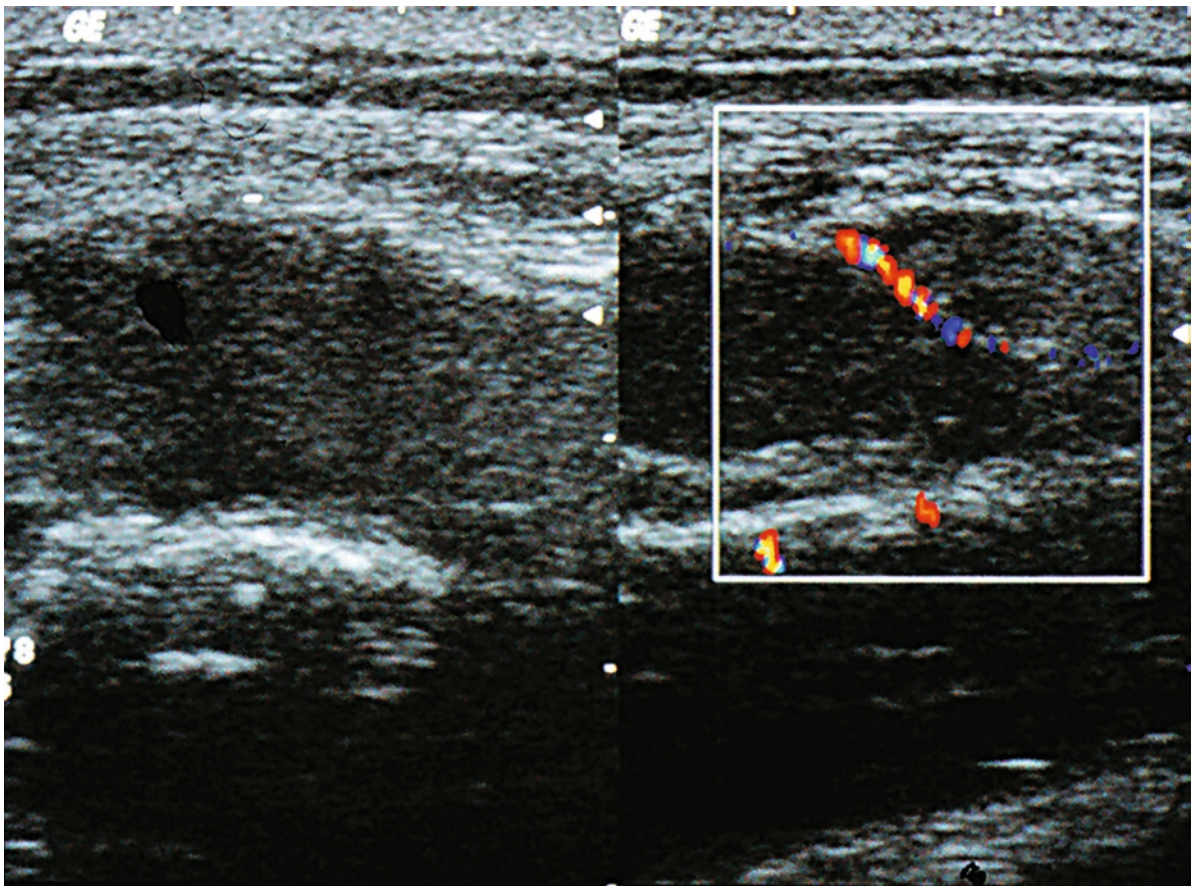

Fig. 2.23 A highly malignant non-Hodgkin's lymphoma invading the ribs, with pathological neoformation of vessels on color-Doppler sonography. The diagnosis was established by sonography-guided aspiration

located close to the transducer head—in a very favorable location for sonographic diagnosis. During ongoing therapy, osteolyses may serve as monitoring parameters for the bony chest in the presence of diseases such as multiple myeloma (Fig. 2.24), small-cell bronchial carcinoma, prostate carcinoma or breast carcinoma. Any increase or decrease in size and any change in the sonomorphological internal structure can be compared and documented. Recalcification under therapy is seen earlier than it is on X-rays.

A peripheral bronchial carcinoma invading the chest wall (Pancoast's tumor) is better assessed by sonography than by computed tomography; the same is true for invasion of the subclavian vessels (Suzuki et al. 1993; Bandi et al. 2008; Figs. 2.25 and 2.26).

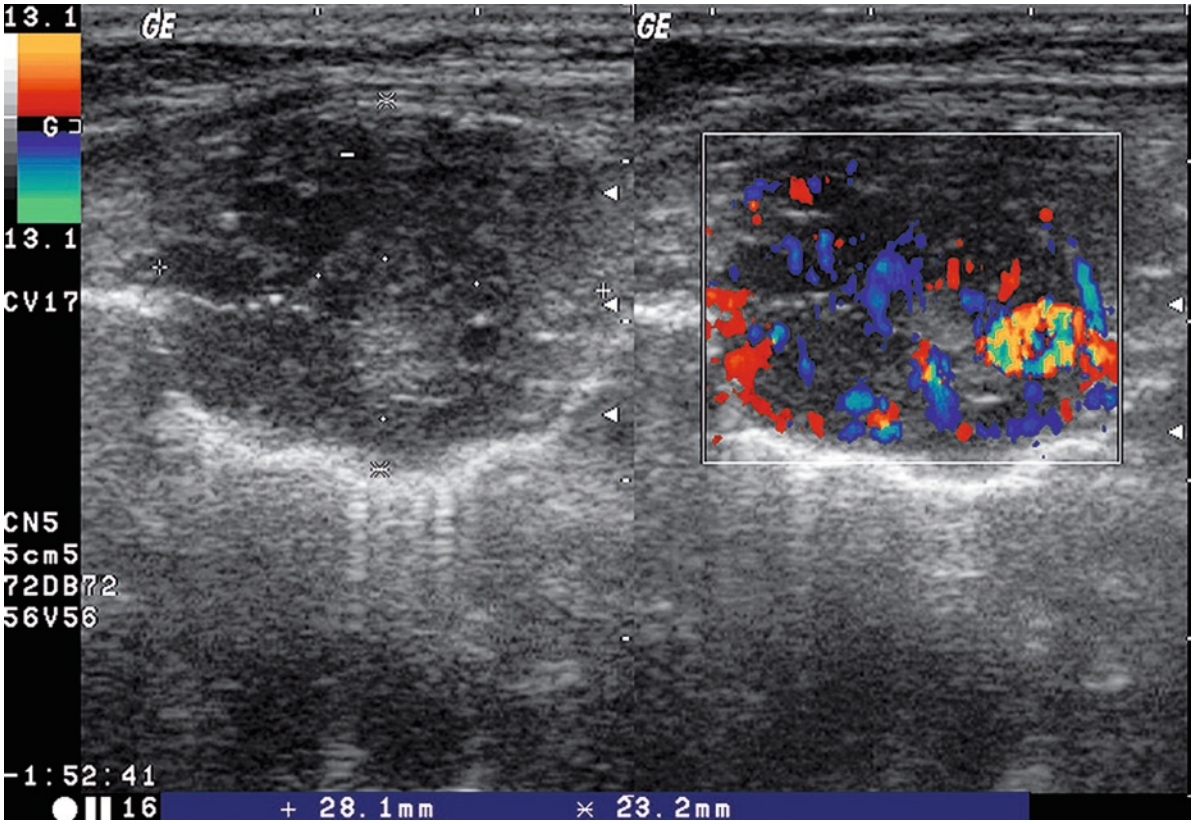

Fig. 2.24 Multiple myeloma with typically strong vascularization. The diagnosis was established by sonography-guided biopsy

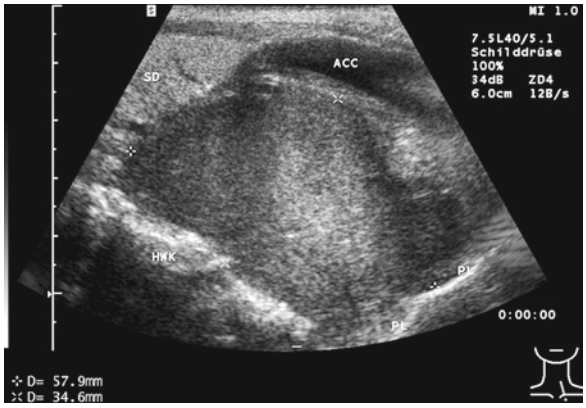

Fig. 2.25 Lung carcinoma growing into the upper aperture of the thorax. *ACC* a. carotis communis

2.3 Summary

Visualization of lymph nodes and cautious assessment of the malignant or benign nature of a lesion is an important indication for sonography of the chest wall. All ambiguous lesions in the chest wall are well accessible to sonography-guided aspiration for histological confirmation of the diagnosis, if such confirmation is required for therapy. The risk of aspiration is very low owing to the favorable location of the lesions. Once malignancy has been proven, the progression of chest wall lesions under therapy can be monitored.

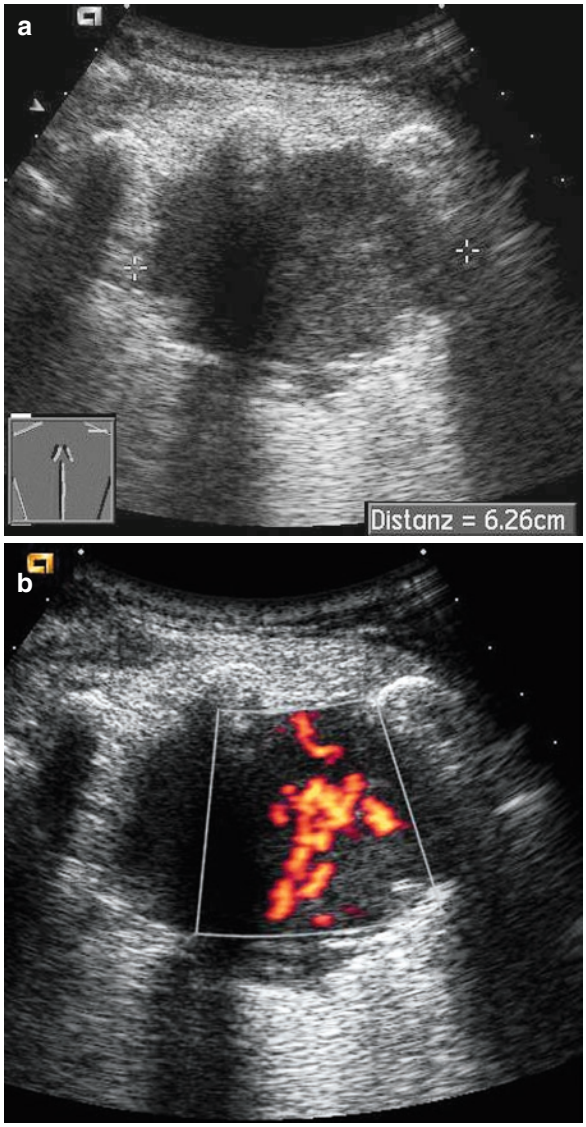

Fig. 2.26 (**a**) Epidermoid carcinoma at the right apex of the lung, in dorsal location, invading the chest wall. (**b**) Irregular vascularization pattern—vascular inferno

Fractures of the ribs as well as the sternum can be visualized well by sonography. Fracture diagnosis by sonography is not only much more sensitive than with conventional X-rays but also allows accompanying soft-tissue lesions, hematomas and pleural effusions to be detected rapidly and reliably.

References

Bandi V, Lunn W, Ernst A, Eberhardt R, Hoffmann H, Herth F (2008) Ultrasound vs. computed tomography in detecting chest wall invasion by tumor: a prospective study. Chest 133:881–886

Bitschnau R, Gehmacher O, Kopf A, Scheier M, Mathis G (1997) Ultraschalldiagnostik von Rippen- und Sternumfrakturen. Ultraschall Med 18:158–161

Bruneton JN, Caramella E, Aubanel D, Hery M, Ettore F, Boublil JL, Picard L (1984) Ultrasound versus clinical examination for axillary lymph node involvement in breast cancer. Ultrasound 153:297

Bruneton JN, Caramella E, Hery M, Aubanel D, Manzino JJ, Picard L (1986) Axillary lymph node metastases in breast cancer: preoperative detection with US. Radiology 158:325–326

Chang DB, Yuan A, Yu CJ, Luh KT, Kuo SH, Yang PC (1994) Differentiation of benign and malinant cervical lymph nodes with color doppler sonography. Am J Roentgenol 162:965–968

Dubs-Kunz B (1992) Sonographische Diagnostik von Rippenfrakturen. In: Anderegg A, Despland P, Henner H, Otto R (eds) Ultraschalldiagnostik '91. Springer, Berlin/Heidelberg/New York/Tokyo, pp 268–273

Dubs-Kunz B (1996) Sonography of the chest wall. Eur J Ultrasound 3:103–111

Fenkl R, Garrel Tv, Knappler H (1992) Diagnostik der Sternumfraktur mit Ultraschall—eine Vergleichsstudie zwischen Radiologie und Ultraschall. In: Anderegg A, Despland P, Henner H, Otto R (eds) Ultraschalldiagnostik '91. Springer, Berlin/Heidelberg/New York/Tokyo, pp 274–279

Friedrich RE, Volkenstein RJ (1994) Diagnose und Repositionskontrolle von Jochbogenfrakturen. Ultraschall Med 15:213–216

Fultz PJ, Feins RH et al (2002) Detection and diagnosis of nonpalpable supraclavicular lymph nodes in lung cancer at CT and US. Radiology 222:245–251

Goeckenjan G, Sitter H, Thomas M et al (2011) Prevention, diagnosis, therapy, and follow-up of lung cancer: interdisciplinary guideline of the German Respiratory Society and the German Cancer Society. Pneumologie 65:39–59

Griffith JF, Rainer TH, Ching AS, Law KL, Cocks RA, Metreweli C (1999) Sonography compared with radiography in revealing acute rib fracture. AJR Am J Roentgenol 173:1603–1609

Gritzmann N, Grasl MC, Helmer M, Steiner E (1990) Invasion of the carotid artery and jugular vein by lymph node metastases: detection with sonography. AJR Am J Roentgenol 154:411–414

Hergan K, Amann T, Oser W (1994) Sonopathologie der Axilla: Teil II. Ultraschall Med 15:11–19

Hergan K, Haid A, Zimmermann G, Oser W (1996) Preoperative axillary sonography in breast cancer: value of the method when done routinely. Ultraschall Med 17:14–17

Leitgeb N, Bodenteich A, Schweighofer F, Fellinger M (1990) Sonographische Frakturdiagnostik. Ultraschall Med 11:206–209

Mariacher Gehler S, Michel BA (1994) Sonography: a simple way to visualize rib fractures (letter). AJR Am J Roentgenol 163:1268

Mathis G (1997) Thoraxsonography—Part I: chest wall and pleura. Ultrasound Med Biol 23:1141–1153

van Overhagen H et al (2004) Metastases in supraclavicular lymph nodes in lung cancer: assessment with palpation. US CT Radiol 232:75–80

Prosch H, Strasser G, Sonka C et al (2007) Cervical ultrasound (US) and US-guided lymph node biopsy as a routine procedure for staging of lung cancer. Ultraschall Med 28:598–603

Riebel T, Nasir R (1995) Sonographie geburtstraumatischer Extremitätenläsionen. Ultraschall Med 16:196–199

Sakai F, Sone S, Kiyono K et al (1990) High resolution ultrasound of the chest wall. Fortschr Röntgenstr 153:390–394

Suzuki N, Saitoh T, Kitamura S (1993) Tumor invasion of the chest wall in lung cancer: diagnosis with US. Radiology 187:39–42

Tschammler A, Ott G, Schang T, Seelbach-Goebel B, Schwager K, Hahn D (1998) Lymphadenopathy: differentiation of benign from malignant disease—color Doppler US assessment of intranodal angioarchitecture. Radiology 208: 117–123

Tschammler A, Beer M, Hahn D (2002) Differential diangosis of lymphadenopathy: power Doppler vs color Doppler sonography. Eur Radiol 12:1794–1799

Walz M, Muhr G (1990) Sonographische Diagnostik beim stumpfen Thoraxtrauma. Unfallchirurg 93:359–363

Wischofer E, Fenkl R, Blum R (1995) Sonographischer Nachweis von Rippenfrakturen zur Sicherung der Frakturdiagnostik. Unfallchirurg 98:296–300

Wüstner A, Gehmacher O, Hämmerle S, Schenkenbach C, Häfele H, Mathis G (2005) Ultraschalldiagnostik beim stumpfen Thoraxtrauma. Ultraschall Med 26:285–290

http://www.springer.com/978-3-642-21246-8

Chest Sonography
Mathis, G. (Ed.)
2011, VII, 249 p., Hardcover
ISBN: 978-3-642-21246-8